Available online at www.sciencedirect.com
SCIENCE DIRECT
Polymer 47 (2006) 2874–2883
polymer
www.elsevier.com/locate/polymer

Ethylene/(meth)acrylic acid ionomers plasticized and reinforced by metal soaps

Katsuyuki Wakabayashi, Richard A. Register *

Department of Chemical Engineering, Princeton University, A423 Engineering Quadrangle, Princeton, NJ 08544-5263, USA

Received 18 December 2005; received in revised form 7 February 2006; accepted 8 February 2006
Available online 2 March 2006

Abstract

Metal soaps, also known as fatty acid salts, resemble oligomers of ethylene/methacrylic or ethylene/acrylic acid (E/(M)AA) ionomers, in that they contain carboxylic salt headgroups and long methylene sequences in their hydrocarbon tails. Such soaps might thus be expected to form miscible blends with E/(M)AA ionomers under suitable conditions, providing a separate route to increasing an ionomer's ion content and modifying its physical properties. We show here that the structure and property modifications induced by blending metal soaps into E/(M)AA ionomers are complex, and depend on both the neutralizing cation and on whether the hydrocarbon tails are crystallizable. In the melt at sufficiently high temperatures, all blends show a coassembled structure, where the salt groups of the soap coaggregate with the salt groups on the ionomer; despite the high ion content of these blends, they retain the melt processability characteristic of neat E/(M)AA ionomers of much lower ion content. Non-crystallizable magnesium oleate and magnesium erucate act as permanent plasticizers, lowering the matrix glass transition temperature. Magnesium stearate, whose alkyl tails easily form a rotator phase, can slowly 'cocrystallize' with ethylene sequences in the ionomers, leading to high moduli; however, primary crystallization is suppressed in these blends. Finally, while sodium stearate is miscible with the ionomers at elevated temperatures, it phase-separates on cooling, prior to crystallization of the ionomer; such blends are essentially composites of pure stearate and ionomer phases, with their associated individual properties, rather than possessing new structures or properties resulting from coassembly.

Keywords: Ionomer; Blend; Metal soap

1. Introduction

Polymers that contain a small percentage of ionic functional groups covalently bound to the chains, termed ionomers, have been widely studied for over four decades [1,2]. Semicrystalline ionomers, specifically those derived from ethylene/methacrylic acid (E/MAA) and ethylene/acrylic acid (E/AA) statistical copolymers, are of particular interest because of their notably high stiffness, abrasion resistance, optical clarity, and adhesion [3]. Many of these properties are tied to the complex nanoscale morphology found in E/(M)AA ionomers, comprising ethylene crystallites, amorphous polymer segments and ionic aggregates [4–6]. One way to tailor the material properties of ionomers is through their ion content, but in practice, the range of achievable properties is hindered by the impractically high viscosity and consequent lack of processability which ensues at moderately high ion contents [7]. Attempts have been made in the past to incorporate small molecules and oligomers to better adjust or even enhance the mechanical properties of ionomers via plasticization [8] of the backbone [9,10] or the ionic regions [9–15] or both [16]. Most of these studies involved amorphous ionomers and non-crystalline plasticizers, although a few blends with crystalline oligomers [15] (fatty acid and metal soap) and semi-crystalline syndiotactic polystyrene ionomers [13] have been reported.

In this paper, we investigate the structure and properties of new ionomer:small molecule blends, based on semicrystalline E/(M)AA ionomers and metal soaps. Metal soaps are the salts of long-chain saturated or unsaturated α-carboxylic acids (fatty acids), typically derived from natural products; here, we employ acids with chain lengths from C_{16} to C_{22}. Their structure and thermal behavior have been extensively investigated since the early 1900s [17]. They are commonly used as soaps and lubricants, and are also added to polymers as heat stabilizers, antiscorching and slip agents [18–20]. There is an obvious structural similarity between E/(M)AA ionomers and metal soaps, since they share both a common functional

* Corresponding author. Tel.: +1 609 258 4691; fax: +1 609 258 0211.
E-mail address: register@princeton.edu (R.A. Register).

0032-3861/$ - see front matter © 2006 Elsevier Ltd. All rights reserved.
doi:10.1016/j.polymer.2006.02.019

group (COO^-M^+) as well as long sequences of CH_2 units. Therefore, these blends are expected to exhibit intimate molecular interactions in each of the ionic, amorphous organic, and crystalline regions, possibly yielding synergistic material property modifications. As we show below, such synergy can indeed be achieved, but its nature and extent are strongly dependent on the nature of both the salt group (choice of metal cation, Na^+ vs. Mg^{2+}) and the fatty acid tail (crystallizable vs. non-crystallizable).

2. Experimental

2.1. Materials

Table 1 lists all the ionomers used in the blends, provided by DuPont, along with information on their compositions; some materials containing a third monomer, *n*-butyl acrylate (*n*BA), are termed 'terpolymer ionomers'. The sample code (e.g. E/8AA/16*n*BA-45Mg) indicates the nature and content of the acid comonomer (8AA = 8 wt% AA) and termonomer, if any (16*n*BA = 16 wt% *n*BA), followed by the neutralizing cation type and level (45Mg = 45% of the acid groups neutralized by Mg^{2+}). The co- and terpolymers are produced by free radical polymerization at high pressure [3], with the acid contents determined by titration and the *n*BA content by infrared spectroscopy. The corresponding ionomers were prepared by subsequent melt neutralization [3], with the neutralization level determined by X-ray fluorescence.

Several metal soaps were employed in this investigation, often prepared in situ by melt coneutralization of technical grade fatty acid with the acid copolymer or terpolymer. Stearic acid (*n*-octadecanoic acid) was obtained from Witco Chemical (Hystrene 9718; 94% stearic acid, 3% palmitic acid (*n*-hexadecanoic acid)). The magnesium stearate (MgSt) discussed in this work was either made in situ from this stearic acid, or was acquired directly as the Mg salt of the same grade of stearic acid (Witco Chemical grade D, 94% MgSt). For comparison, we also employed a stearic–palmitic acid blend (J.T. Baker Triple Pressed, min. 40% stearic, min. 40% palmitic, min. 90% stearic and palmitic together); the metal soap generated in situ by neutralizing this fatty acid blend is denoted MgStPm. Finally, sodium stearate (NaSt) was acquired and used as such (Witco Chemical grade EA, 62–72 wt% NaSt, 25–32 wt% NaPm). The unsaturated acids employed were technical grade oleic acid (*cis*-9-octadecenoic acid; Aldrich, 90%) and erucic acid (*cis*-13-docosenoic acid; Pfaltz and Bauer, 90%); the soaps generated in situ by neutralization of these fatty acids are denoted MgOl and MgEr, respectively. Ex situ specimens of higher-purity MgOl and MgEr for phase behavior studies were prepared by completely neutralizing the corresponding pure grade fatty acids (from Sigma-Aldrich, 99+% purity) with the stoichiometric amount of dibutyl magnesium (dissolved in heptane) in tetrahydrofuran solution. All data presented herein were acquired on the anhydrous forms of the metal soaps, which were obtained by drying in a vacuum oven at 95 °C for more than 24 h.

The preparation of ionomer:metal soap blends was carried out at DuPont by melt mixing. Ionomers and blends based on the rubbery terpolymer (E/9AA/45*n*BA) were prepared in a Haake mixer, heating to 230 °C; the feeds consisted of acid terpolymer, fatty acid, and sufficient $Mg(OH)_2$ to produce stoichiometric neutralization of all acid functional groups present. The absence of an X-ray diffraction peak corresponding to $Mg(OH)_2$ confirmed complete reaction. Blends based on the other (semicrystalline) acid co- and terpolymers were prepared by twin-screw extrusion, with a maximum zone temperature of 230–250 °C. For the Mg-neutralized blends, the feeds again consisted of acid copolymer or terpolymer, fatty acid, and sufficient $Mg(OH)_2$ to produce stoichiometric neutralization of all acid functional groups present. However, the presence of a small X-ray diffraction peak from $Mg(OH)_2$, and a small infrared stretch near 1696 cm^{-1} from –COOH, indicated that reaction was not entirely complete by the time the material reached the die. The 65:35 blend of E/8AA/16*n*BA with MgSt was intentionally neutralized to 114% of stoichiometric, and showed the largest X-ray diffraction peak from residual $Mg(OH)_2$. For the Na ionomer blend, the feeds consisted of a partially-neutralized ionomer (E/19MAA-37Na), NaSt, and sufficient Na_2CO_3 dispersed in a carrier resin (E/10MAA) to bring the material to 95% of stoichiometric

Table 1
Characteristics of ethylene-based ionomers studied

Ionomer	Mole fraction ethylene	Equivalent weight (g/equiv.)[a]	Peak E'' (°C)[b]	Peak T_{m1} (°C)[c]	Peak T_{m2} (°C)[c]	Weight fraction crystallinity at 25 °C[c]	Young's Modulus E at 25 °C (MPa)[c]
E/9AA/45*n*BA-80Mg[d]	0.773	780	−45	None	None	0	20
E/8AA/16*n*BA-45Mg	0.919	850	−24,48	78	52	0.17	120
E/19MAA-37Na	0.929	450	−52,47	86	46	0.15	520
E/12AA-62Mg	0.947	580	−14,52	98	50	0.16	330

[a] Expressed for the acid copolymer or terpolymer on which the ionomer is based.
[b] Loss modulus maxima after 8–10 days of room-temperature aging following a quench from the melt.
[c] After 5–6 days of room-temperature aging following a quench from the melt; T_{m1} and T_{m2} are the peak temperatures for melting of primary and secondary crystallites, respectively; crystallinities calculated by DSC with $\Delta H = 278$ J/g for the perfect crystal [21].
[d] *n*BA content estimated based on monomer feed and known reactivity ratios.

neutralization. However, the presence of minute X-ray diffraction peaks from Na_2CO_3 also indicated the presence of trace unreacted Na_2CO_3.

Blend compositions were calculated from the feeds, and are expressed as the weight ratios of ionomer:metal soap in the final product, which differs slightly from the feed ratios of the organics, due to the increase in molecular weight upon neutralization. While some blend series were prepared at varying weight ratios of ionomer:metal soap, the property changes were found to be roughly linear in metal soap content and were generally modest below 20 wt% soap. Consequently, the results reported herein are limited to blends containing 35–41 wt% soap (nominally 40 wt%).

For testing, the ionomers and blends were melt-pressed into 0.2–0.5 mm thick sheets at 150 °C using a PHI hot press, followed by a quench to room temperature. The molded sheets were stored under vacuum or in a desiccator over dry $CaSO_4$ at room temperature for varying aging times.

2.2. Measurements

The nanometer-scale morphology of the blends was probed by small-angle X-ray scattering (SAXS), employing Cu Kα radiation from a PANalytical PW3830 X-ray generator; an Anton Paar compact Kratky camera with a custom hotstage for precise temperature control [22]; and an MBraun OED-50M position sensitive detector. The data reduction procedure for SAXS, leading to desmeared absolute intensity I/I_eV vs. the magnitude of the scattering vector q, has been described previously [23]. Wide-angle X-ray diffraction employed the same generator, a Philips-Norelco wide-range goniometer (run at $2\theta = 1°$/min), retrofitted with an Advanced Metals Research graphite focusing monochromator for the diffracted beam, and a Philips Electronic Instruments scintillation detector. Thermal characterization was performed on a Perkin–Elmer DSC-7 equipped with an intracooler and calibrated with indium and tin. Pyris 1 software was used for data acquisition (heating ramp of 10 °C/min) and analysis (melting point and heat of melting determination). Five to ten milligrams specimens were prepared in volatile aluminum pans either from the molded sheets described above or directly from dried metal soap powder. For dynamic mechanical thermal analysis (DMTA), 4–5 mm × 35 mm specimens were cut from a molded sheet and tested in either a Rheometrics RSA-II or a TA Instruments RSA-3 equipped with liquid nitrogen cooling, at a frequency of 1 Hz with 0.2% strain amplitude and 3 °C temperature steps. Tensile stress–strain testing was carried out at 25 °C on ASTM D1708 dogbones stamped from the molded sheets, using an Instron Model 1122 with environmental chamber providing ±0.3 °C temperature control. The crosshead speed was 2 in./min (initial strain rate of 0.038 s^{-1}) and the compliance of the load cell and grips was corrected for during data reduction. The Young's modulus E was obtained as the small-strain (<5%) slope of the curve. Melt index measurements (ASTM D1238 Condition E, at 190 °C) [24] were conducted at DuPont on selected ionomers and blends.

3. Results and discussion

The ionomers employed in this study are described briefly in Table 1. Their crystallinities range from zero (at the lowest ethylene content) up to the value of ca. 20% typical for E/(M)AA ionomers. The equivalent weight of the acid co- and terpolymers is a measure of the potential ion content of the ionomers (at full neutralization); the equivalent weights (molecular weights) of the fatty acids employed here are lower, 256–339 g/mol. So the incorporation of 40 wt% of metal soap, coupled with complete neutralization of the material, yields an ion content 2–4 times larger in the blends than in the unmodified ionomers.

As a preliminary mechanical property assessment, we conducted room temperature tensile testing on selected materials at various times after quenching from the melt. Pure E/(M)AA ionomers exhibit a significant dependence of the Young's modulus E on the time of aging or storage at room temperature, due to the slow formation of secondary crystals [25]; we anticipated a similar phenomenon with the ionomer:metal soap blends. Fig. 1 shows E vs. aging time for

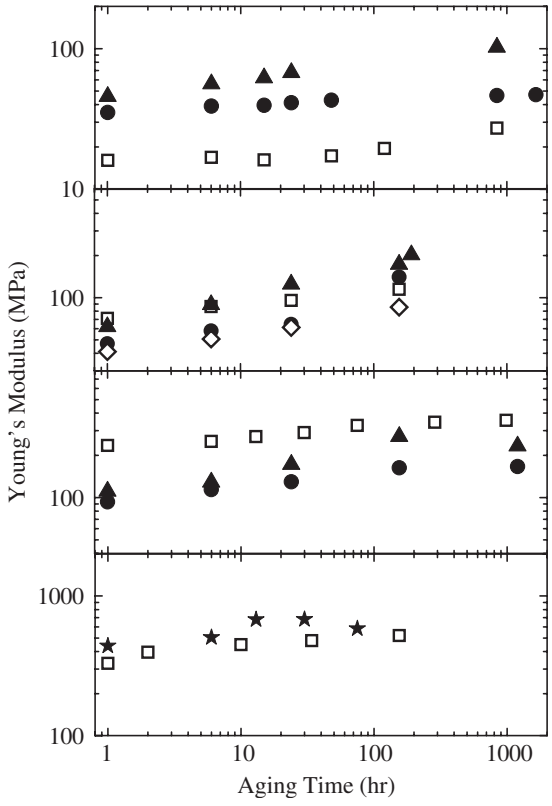

Fig. 1. Young's modulus of ethylene-based ionomers and their blends with metal soaps plotted as a function of room temperature aging time. The ionomers are neutralized only partially, as indicated below; the blends are nominally 100% neutralized. Top panel: (□) E/9AA/45*n*BA-80Mg ionomer, (●) 59:41 ionomer:MgOl blend, (▲) 59:41 ionomer:MgStPm blend. Second panel: (□) E/8AA/16*n*BA-45Mg ionomer, (●) 59:41 ionomer:MgOl blend, (◇) 60:40 ionomer:MgEr blend, (▲) 65:35 ionomer:MgSt blend. Third panel: (□) E/12AA-62Mg ionomer, (●) 60:40 ionomer:MgOl blend, (▲) 60:40 ionomer:MgSt blend. Bottom panel: (□) E/19MAA-37Na ionomer, (★) 61:39 ionomer:NaSt blend.

the four different blend systems used in this study. All materials show a general trend of increasing E upon aging, with the increase continuing even after a month. However, the magnitude and rate of modulus change varies greatly from system to system. For example, close inspection of the top three panels in Fig. 1 reveals that blends with magnesium stearate (MgSt) or a stearate–palmitate mix (MgStPm) consistently show a stronger dependence of E upon aging time than either the pure ionomers, or blends with the salts of unsaturated fatty acids (magnesium oleate, MgOl, and magnesium erucate, MgEr). The microscopic origins of these modulus changes are revealed below, in sections divided according to the different metal cations and fatty acid types employed, each of which shows qualitatively different phenomena. Section 3.1 examines blends with MgOl and MgEr; Section 3.2 examines blends with MgSt and MgStPm; and Section 3.3 examines blends with sodium stearate, NaSt.

3.1. Simple plasticization: ionomers blended with MgOl or MgEr

The salts of unsaturated fatty acids, usually derived from plant oil, have been studied far less than their animal fat-based saturated analogs. To investigate their phase behavior, pure MgOl and MgEr were synthesized from the corresponding acids and characterized by DSC and X-ray scattering. Room temperature X-ray diffraction profiles [26] of both MgOl and MgEr exhibited a broad hump around $2\theta = 20°$, characteristic of a liquid-like packing of the hydrocarbon tails [27]. Both materials showed two broad peaks at small angles [26], in a q-ratio of approximately 1:2, reflecting a disordered mesophase structure generally similar to that known for MgSt above 190 °C [26,28]; the characteristic spacing measured for MgEr ($d = 3.5$ nm) is larger than that for MgOl ($d = 3.1$ nm), due to the differences in tail length (C_{22} vs. C_{18}). DSC showed no endothermic peaks for either material between 0 and 250 °C, suggesting that no phase transitions occur in the temperature range of interest and that both MgOl and MgEr can be considered as simple non-crystalline amphiphiles.

We first examined the effect of blending a non-crystalline soap into a non-crystalline ionomer derived from E/9AA/45nBA; the high content of nBA completely eliminates crystallinity in ionomers derived from this terpolymer, as confirmed by DSC and X-ray diffraction [26]. The unmodified ionomers neutralized 50 and 80% with Mg^{2+} both show glass transition temperatures $T_g = -40$ °C, taken as the DMTA E'' peak temperature (Fig. 2). The DMTA curves for a 59:41 blend of E/9AA/45nBA with MgOl (fully neutralized) are shown as well, from which it is readily seen that MgOl acts as an effective plasticizer, lowering the T_g by 25 °C even when compared with the partially-neutralized neat ionomer. Fig. 2 also shows that the storage modulus above T_g increases steadily on going from 50% neutralized ionomer to 80% ionomer to 100% neutralized blend; such a trend is expected if we simply consider the ionic aggregates as crosslinks, since increasing neutralization thus leads to a progressive decrease of the molecular weight between crosslinks [6]. However, there is no

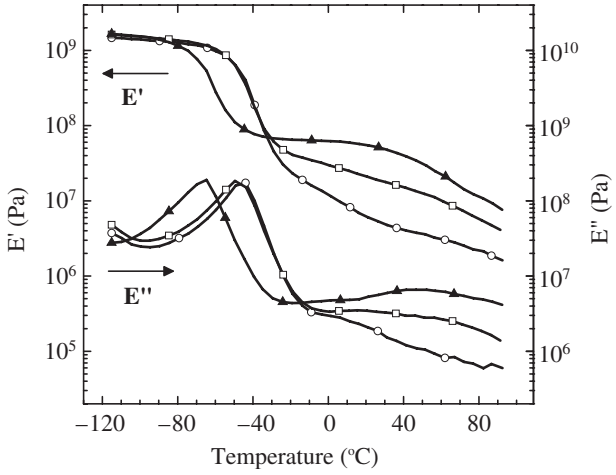

Fig. 2. Dynamic storage (E') and loss (E'') moduli vs. temperature obtained from DMTA at 1 Hz; samples stored at room temperature for 8 days prior to testing. (○) E/9AA/45nBA-50Mg, (□) E/9AA/45nBA-80Mg, (▲) 59:41 ionomer:MgOl blend, fully neutralized.

obvious effect of the MgOl on the magnitude of the rubbery plateau modulus, beyond what would be anticipated for a fully-neutralized ionomer with no metal soap added.

There is, however, a major impact of the MgOl on the melt viscosity of the ionomer, as measured through the melt index (MI), which is inversely related to melt viscosity. The 50%-neutralized ionomer has MI = 1.4 g/10 min, while the 80%-neutralized ionomer has MI < 0.1 g/10 min, considered to be essentially 'no flow'; higher neutralization levels were not possible through melt processing. But the 100%-neutralized, 59:41 ionomer:MgOl blend shows MI = 6.7 g/10 min, which is the value expected for a 30%-neutralized ionomer with no metal soap added. So here, the addition of MgOl yields a fully-neutralized material with a broad and nearly flat rubbery plateau (Fig. 2), while preserving the melt processability typically associated only with low ion contents [7,29,30]. This result is similar to that found when zinc stearate is employed as a plasticizer for zinc-neutralized sulfonated ethylene–propylene–diene terpolymer, as reported previously by Makowski et al. [31]. While a detailed study of the melt rheology of ionomer:metal soap blends is beyond the scope of the present report, note that all the blends prepared in this work have melt indices conducive to melt processing (indeed, all the blends were prepared by melt processing), despite their uniformly high ion contents.

Fig. 3 compares the SAXS pattern of the 41 wt% MgOl-modified E/9AA/45nBA ionomer with those of the pure components. As noted above, MgOl shows two relatively broad peaks in a q-ratio of 1:2, implying a disordered mesophase structure with $d = 3.1$ nm. The ionomer shows only a very broad and weak peak near $q^* \approx 2.5\ nm^{-1}$ due to scattering from the ionic aggregates [32]. The SAXS pattern for the blend is qualitatively intermediate between the two, with a single broad peak at $q^* = 2.1\ nm^{-1}$. This intermediate SAXS profile indicates that the ionic aggregates present in the blend contain carboxyl groups from both the salt and the

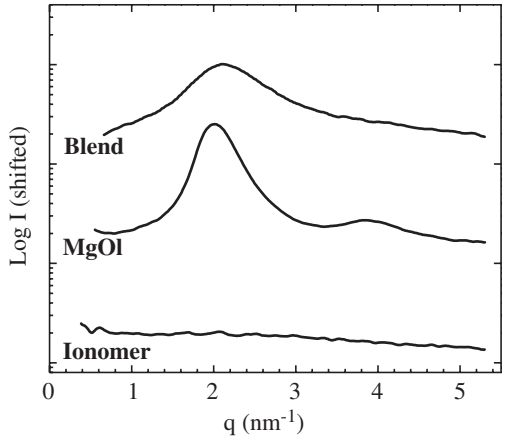

Fig. 3. Room-temperature SAXS profiles of E/9AA/45*n*BA-80Mg ionomer, pure MgOl, and the fully-neutralized 59:41 blend; blend and ionomer stored for 3 days prior to measurement. The abscissa is the scattering vector magnitude $q=(4\pi/\lambda)\sin\theta$, where λ is the wavelength of the X-rays and θ is half the scattering angle. Each curve is shifted vertically by a decade for easy comparison.

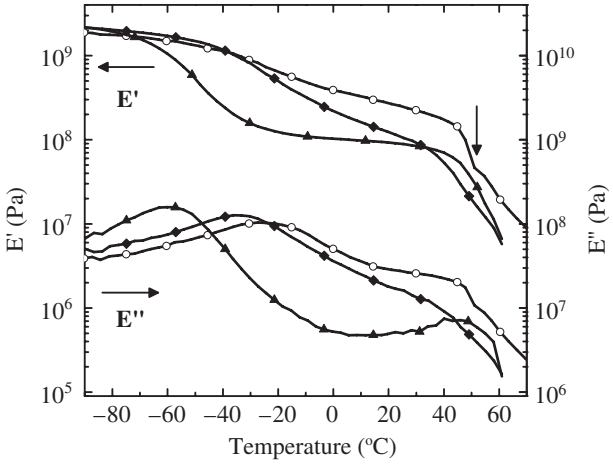

Fig. 4. Dynamic storage (E') and loss (E'') moduli vs. temperature obtained from DMTA at 1 Hz; samples stored at room temperature for 8 months prior to testing. (○) E/8AA/16*n*BA-45Mg, (♦) 59:41 ionomer:MgOl blend, fully neutralized, (▲) 60:40 ionomer:MgEr blend, fully neutralized. The arrow highlights the two-step modulus drop for the unmodified ionomer.

ionomer [12,14]. The ionomer and MgOl are intimately mixed, rather than being phase-separated, which is consistent with the transparent appearance of the samples and the plasticization effect noted in Fig. 2; no tendency towards demixing was ever observed at any temperature. Thus, blending a non-crystalline Mg soap with a non-crystalline Mg ionomer yields an intimate blend, where the soap's salt headgroups coassemble into the ionic aggregates, while its hydrocarbon tails plasticize the matrix; we refer to these coassembled entities as 'ionic coaggregates' in what follows.

However, typical E/(M)AA ionomers are semicrystalline, with crystallinities depending on the content of acid comonomer (and termonomer, if any), as shown in Table 1. This crystallinity has a major impact on the structure and mechanical properties of E/(M)AA ionomers, through both the primary crystals which form immediately upon cooling, and on the thinner secondary crystals which develop slowly after primary crystallization, during storage at room temperature. These secondary crystals, which form within the amorphous layers separating the primary crystals, serve to reinforce these amorphous layers [6,33]. Blending MgOl or MgEr into such semicrystalline ionomers is expected to yield more complex behavior compared with the fully-amorphous case just considered. Indeed, Fig. 1 shows that blending MgOl or MgEr into semicrystalline E/8AA/16*n*BA (second panel) and E/12AA (third panel) ionomers leads to a lower modulus, even though the blends are fully neutralized, while the unmodified ionomers are only partially neutralized.

Fig. 4 shows DMTA data for the E/8AA/16*n*BA-based materials, stored for an extended period at room temperature prior to testing. As found for the amorphous ionomers in Fig. 2, adding ≈40 wt% MgOl again plasticizes the material, dropping T_g (E'' peak) by 10 °C; the longer-chain MgEr is an even more effective plasticizer, reducing T_g by more than 30 °C. Yet Fig. 1 shows that aging at room temperature leads to a progressive increase in modulus in these blends, which we anticipate is due to secondary crystallization. To confirm this, we examined how the DSC trace for the E/12AA ionomer, blended 60:40 with MgOl, changed following different periods of room-temperature aging after a quench from the melt, as presented in Fig. 5. The '0 h' trace shows that primary crystals do form immediately upon cooling in this blend, but the enthalpy of this peak is only about 30% that of the pure ionomer quenched and reheated similarly, though the ionomer constitutes 59 wt% of the blend. This indicates a substantial but incomplete suppression of primary crystallization by the MgOl; the sequences which failed to crystallize initially can thus participate in slow secondary crystallization subsequently. This process is revealed in Fig. 5 by the blend thermograms at longer storage times, where a prominent secondary crystallization peak develops. After 10 days, this peak has an area

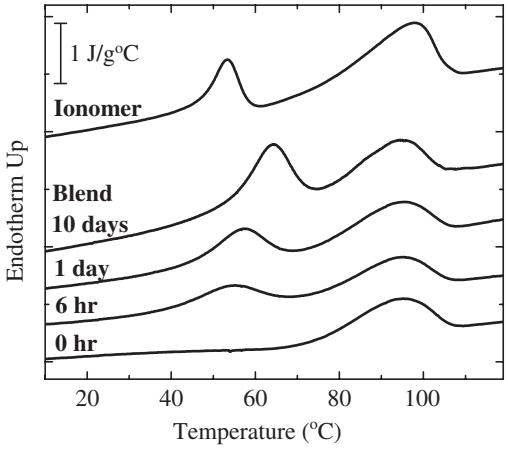

Fig. 5. DSC thermograms of the fully-neutralized 60:40 E/12AA ionomer: MgOl blend, following a quench from 150 °C and aging for various times at room temperature. The top curve is a heating trace for the unmodified E/12AA-62Mg ionomer after aging for 10 days, scaled by 0.6 (=weight fraction of ionomer in blend). The curves are shifted vertically for easy comparison.

comparable to that of the endotherm corresponding to the primary crystals, and the total heat of fusion is 56% of that of the unmodified ionomer aged similarly, nearly matching the ionomer's content in the blend. Note also that the melting point of these crystals in the blend after 10 days of aging (64 °C) is significantly higher than for the secondary crystals in the pure ionomer (53 °C), because in the blend, a larger fraction of the longer sequences fail to crystallize during primary crystallization, and can thus yield higher-melting secondary crystals. This pronounced secondary crystallization process accounts for the stronger dependence of the blend's modulus on aging time, as compared with the pure ionomer (Fig. 1, third panel); however, even after extended aging, the blend's modulus is still only about half the unmodified ionomer's modulus. Thus, in this case, the lower crystallinity in the blend—which contains 41 wt% non-crystallizable diluent, MgOl—has a stronger impact on the modulus than the higher neutralization level (62% for the unmodified ionomer, 100% for the blend).

The formation and melting of these secondary crystals can be directly observed by SAXS, as shown in Fig. 6 for a well-aged E/8AA/16*n*BA ionomer blended with 40 wt% MgEr. The corresponding DSC trace, shown in the inset, reveals a well-developed secondary crystal peak at 66 °C; in this case, the primary crystal melting peak (near 80 °C) is depressed in both temperature and area (relative to the E/12MAA ionomers in Fig. 5) because of the incorporation of 16 wt% *n*BA termonomer statistically along the chain. At room temperature, the SAXS profile shows a major peak at $q^* = 1.7\ \mathrm{nm}^{-1}$ from the ionic coaggregates, as well as a minor peak near $q^* = 0.6\ \mathrm{nm}^{-1}$ from polyethylene crystallites; the low-q peak disappears upon heating to 90 °C, consistent with final melting of the crystals as shown by the DSC trace. However, when the crystals melt, the 'ionomer peak' near $2\ \mathrm{nm}^{-1}$ shifts to higher q, implying a reduction in the average separation between ionic aggregates; this is opposite to the behavior of unmodified ionomers [34], where crystal melting causes a shift of the peak

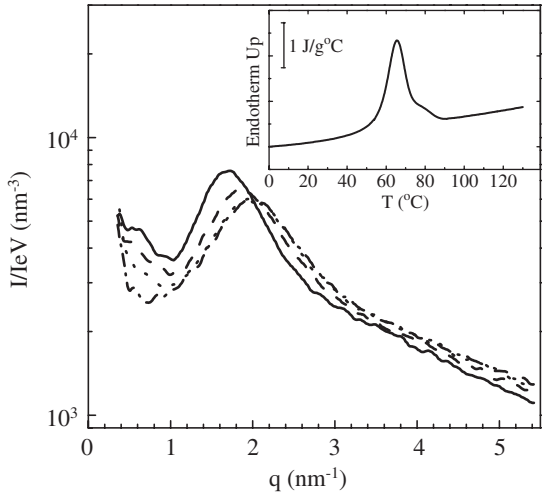

Fig. 6. SAXS profiles taken on heating the fully-neutralized 60:40 E/8AA/16*n*BA ionomer: MgEr blend, following 2 months of room-temperature aging. (—) 25 °C, (– –) 60 °C, (- - - -) 80 °C, and (– -) 90 °C. Inset: DSC trace of the same blend, after 8 months of room-temperature aging.

to lower q. Consequently, melting of the crystals is also accompanied by a significant rearrangement of the coassembled ionic aggregates, leading to more numerous aggregates with a smaller average spacing.

These structural changes upon blending with MgOl and MgEr are also reflected in the DMTA curves in Fig. 4. The unmodified ionomer shows a two-step relaxation over the range 40–70 °C; as reported previously [6], the first (sharp) step reflects the melting of secondary crystallites, while the second (gradual) step reflects devitrification of polymer chain segments surrounding the ionic aggregates. Though the secondary crystals are a minor fraction of the total material, their melting produces a large modulus drop because this event disrupts the pathways of 'hard' material (ionic aggregates plus secondary crystallites) which percolate throughout the amorphous phase at lower temperature [6,12]. In the blends with MgOl and MgEr, only a single DMTA transition can be seen in this range, associated with the melting of the secondary crystals. The MgOl or MgEr effectively plasticizes the polymer chains surrounding the ionic aggregates, so no 'regions of restricted mobility' [35] are present; thus, when the secondary crystals melt, the material is reinforced only by the sparse network of primary crystals, yielding a very low modulus.

In summary, non-crystallizable metal soaps act as plasticizers in two ways: first in the conventional way, by lowering the matrix T_g, and second by preventing the formation of a percolated hard phase which would otherwise form through the overlap of regions of restricted mobility surrounding the ionic aggregates [12]. Previously, such dual behavior from a single plasticizer has been achieved only with relatively volatile plasticizers [16] which partition into both the matrix and ionic-rich regions. By contrast, the ionomer:metal soap blends are quite stable to loss of plasticizer; not only is the metal soap essentially non-volatile, but the formation of ionic coaggregates keeps the soap uniformly dispersed throughout the material, as confirmed by the lack of blooming after long storage times.

3.2. Cocrystallization: ionomers blended with MgSt or MgStPm

The behavior of MgSt and MgStPm has been extensively studied in the past, due to their widespread use in pharmaceutical formulations [19,27,36]. Their phase behavior is more complicated than that of MgOl or MgEr, because these saturated-chain salts are capable of crystallization, and can also exist in at least three structurally distinguishable hydration states (anhydrate, dihydrate, trihydrate) [37]. Since, all our blends are prepared by melt processing at 230 °C or above, the anhydrate is the most relevant for our work. However, even confining our attention to the anhydrate, we find that the transitions from solid through liquid crystalline states to isotropic melt are practically irreversible on cooling. Therefore, two different states of bulk MgSt are possible at room temperature, depending on the processing history: (1) if MgSt is obtained by neutralizing stearic acid in solution (to form the dihydrate) and dried at 100 °C or below (to form the

anhydrate), a lamellar mesostructure is obtained with a bilayer spacing of $d = 5.2$ nm ($q^* = 1.2\ \text{nm}^{-1}$) and a poorly-crystalline packing of the alkyl tails, or (2) if the same material is heated above 120 °C and then cooled, a quenched hexagonal mesostructure is obtained [27,28], with a minor proportion of quenched disordered phase (which is the equilibrium structure above 190 °C) [27,28]. The poorly-ordered crystalline packing observed in case 1 corresponds to the 'rotator' structure [27] commonly observed for alkanes and similar compounds, where the alkyl chains are extended and have a lateral hexagonal packing, but no rotational order [38]. In case 2, the alkyl tails in quenched specimens gradually evolve to a more ordered arrangement (rotator structure) with time as shown below, but the hexagonal mesostructure appears frozen on any reasonable timescale, and does not evolve to the lamellar mesostructure obtained from the initial preparation [26]. Again, since all the ionomer:metal soap blends were melt processed at 230 °C or above, the latter of these two structures is more relevant to the present discussion.

We first investigated the effects of blending a crystallizable metal soap into the amorphous ionomer derived from E/9AA/45*n*BA. Fig. 7 (top) shows the DSC thermogram for MgSt heated previously to 150 °C, which has the hexagonal mesostructure; the endotherm at 50 °C reflects the melting of the partially-ordered alkyl tails to a disordered state [26]. MgSt and MgPm freely cocrystallize, with no substantial dependence of this transition on St:Pm ratio [27], so MgSt and MgStPm can be used interchangeably for our purposes. Recall from Fig. 1 (top panel) that a slow but significant increase in stiffness in the MgStPm-modified E/9AA/45*n*BA ionomer resulted in a Young's modulus value four times as high as that of the pure ionomer after 35 days of aging. Based on the results of the preceding section, an obvious potential cause for this modulus increase is slow crystallization. DSC thermograms for the blend are shown in Fig. 7 (lower portion) following various durations of room-temperature aging. The blend's thermogram

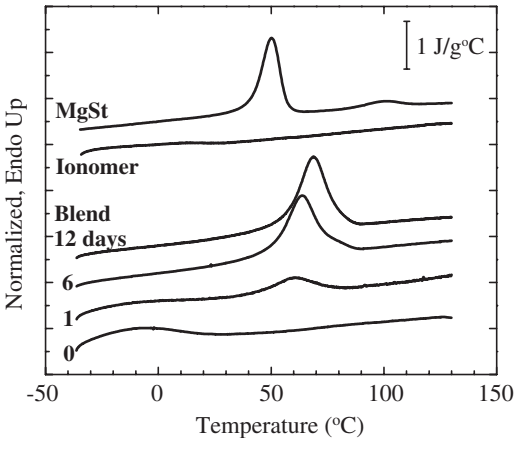

Fig. 7. Bottom: DSC thermograms of the fully-neutralized 59:41 E/9AA/45*n*BA ionomer:MgStPm blend; number next to each curve refers to days of room-temperature annealing following the quench from 150 °C. Top: heating traces for the reference materials (E/9AA/45*n*BA-Mg80 and MgSt), scaled by their respective weight fractions in the blend. The ionomer was aged for 12 days, and MgSt for 6 days, after heating to 150 °C.

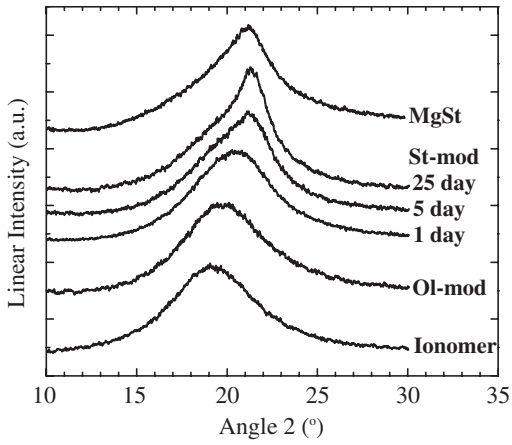

Fig. 8. Center ('St-mod'): X-ray diffraction patterns of the fully-neutralized 59:41 E/9AA/45*n*BA ionomer:MgSt blend, taken after heating to 150 °C, cooling to room temperature, and aging for 1, 5, and 25 days. Note the progressive development of the peak at $2\theta = 21.3°$ characteristic of the rotator phase, which is also present in bulk MgSt (top profile, after heating to 150 °C, quenching to room temperature, and 6 days of room temperature aging). Neither the unmodified E/9AA/45*n*BA-80Mg ionomer, nor its 59:41 blend with MgOl, exhibit this peak (bottom two profiles, after heating to 150 °C, cooling, and 25 days of room-temperature aging). Curves are offset vertically for clarity.

is essentially featureless immediately after quenching from the melt, but gradually develops an endotherm at around 50 °C with aging time. Fig. 8 presents X-ray diffraction data on this same blend following various durations of room-temperature aging, showing the progressive development of a narrower component near $2\theta = 21.3°$ on the broad amorphous halo, characteristic of the rotator phase in MgSt [27]. This peak is not present in the unmodified ionomer, or in its blend with MgOl, even after extended aging, but is clearly evident in bulk MgSt heated to 150 °C, then cooled to and aged at room temperature.

Returning to Fig. 7, in bulk MgSt, the 'melting' of this rotator phase (complete disordering of the alkyl tails) is observed by DSC at 50 °C. In the blend, however, the DSC peak is at significantly higher temperature (70 °C); moreover, after 12 days of aging, its enthalpy corresponds to 58% of the latent heat of melting of neat MgSt with the same thermal history (recall that the blend contains only 40% MgStPm). Thus, we suggest that in the blend, the ordered (rotator-like) alkyl packings which form contain not only the MgStPm tails, but also longer sequences of ethylene units from the ionomer. Such cocrystals are obviously possible only in ionomers having long runs of methylene units, such as ethylene-based ionomers, and not in amorphous ionomers or in crystallizable ionomers whose crystal lattice is incompatible with the rotator structure.

Fig. 9 shows how the SAXS profile of this blend evolves with room temperature aging. Initially, it shows a peak at $q^* = 2.0\ \text{nm}^{-1}$, essentially identical to that from the MgOl-modified ionomer shown previously in Fig. 3. Stearic acid and oleic acid are both C_{18} acids, and the two blends have the same metal soap content, so this similarity is entirely expected if the MgStPm is wholly amorphous upon quenching from the melt. But with aging time at room temperature, the peak shifts progressively and substantially to lower q, which we interpret

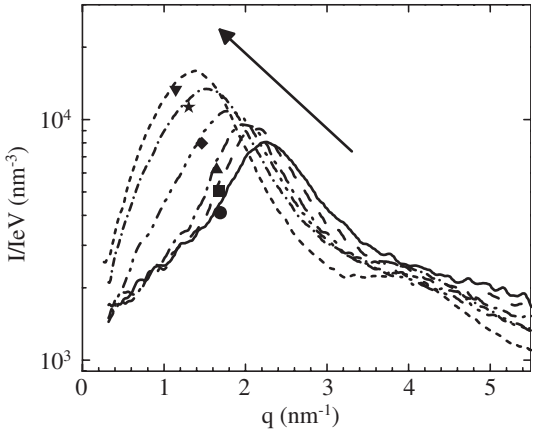

Fig. 9. SAXS profiles of the fully-neutralized 59:41 E/9AA/45*n*BA:MgStPm blend, taken upon cooling from 150 °C and subsequent room-temperature aging. (●) 150 °C, (■) 80 °C, (▲) 25 °C, (♦) 25 °C after 1 h, (★) after 1 day, and (▼) after 7 days. The arrow indicates the direction of movement of the SAXS peak upon room-temperature aging.

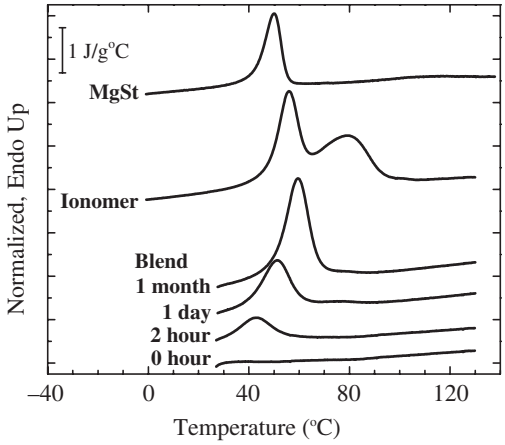

Fig. 10. Bottom: DSC thermograms of the fully-neutralized 60:40 E/8AA/16*n*BA ionomer:MgSt blend; time next to each curve refers to the period of room-temperature annealing following the quench from 150 °C. Top: heating traces for the pure components, scaled by their respective weight fractions in the blend. The ionomer has been aged for 5 months, and MgSt for 20 days, after heating to 150 °C.

as a rearrangement of the mesostructure driven by increased ordering of the hydrocarbon segments. These are not 'crystals' in the same sense as those in, for example, the blend of E/8AA/16*n*BA ionomer with MgOl whose SAXS pattern was shown in Fig. 6; there, the crystals are of the usual plate-like lamellar habit formed by bulk ethylene copolymers. Yet the gradual formation of these rotator-like structures in the MgStPm-modified blend is still sufficient to produce the large modulus increase observed in Fig. 1.

The question then arises as to the behavior of blends of MgSt with ionomers which are themselves capable of crystallization, such as the E/8AA/16*n*BA and E/12AA ionomers. Above the melting point of the unmodified ionomer, the SAXS patterns for all such blends (data not shown) resemble the 150 °C pattern in Fig. 9, with a single peak at $q^* \approx 2\ \mathrm{nm}^{-1}$ reflecting the same ionic coaggregates discussed previously. DSC thermograms of MgSt-modified E/8AA/16*n*BA in Fig. 10 show that upon initial quenching, the blend is entirely amorphous. When the more crystalline E/12AA ionomer was blended with 40 wt% MgSt, a very small endotherm (at 92 °C) could be discerned upon immediate reheating following the initial quench—but very small indeed, amounting to only 2% of that in the pure ionomer (rather than the 60% expected for no suppression) [26]. Recall that some suppression of primary crystallization was observed with MgOl (Fig. 5 and associated discussion); however, this effect is clearly much more pronounced with MgSt. The ability to completely suppress primary crystallization in an ethylene copolymer is truly remarkable. Of course, these ethylene sequences are then available for subsequent secondary crystallization upon room-temperature aging, and Fig. 10 shows that within 2 h a substantial population of crystals has formed. The endotherm corresponding to the melting of these crystals progressively increases in both temperature and enthalpy with further aging.

These secondary crystals exert a substantial influence on the blends' mechanical behavior as well. Fig. 11 compares the DMTA curves for the E/8AA/16*n*BA-45Mg ionomer (same data set as in Fig. 4) with that for its MgSt-modified version, both after 8 months of aging. As already shown for MgOl and MgEr, MgSt can plasticize the matrix, lowering the ion-depleted amorphous domain T_g by approximately 14 °C. While the unmodified ionomer shows the two-step relaxation over 40–70 °C as already discussed, the MgSt ionomer shows only a single step near 60 °C, in common with the ionomers modified with MgOl and MgEr (Fig. 4). The origin of this transition is common to both cases—the melting of secondary crystals—but its magnitude differs considerably when a crystallizable vs. non-crystallizable metal soap is used. At 40 °C, the blend with MgSt shows a storage modulus $E' \approx 300$ MPa (Fig. 11), while the blends with MgOl and MgEr show $E' \approx 100$ MPa (Fig. 4). When MgSt is the soap, both ethylene sequences and the alkyl

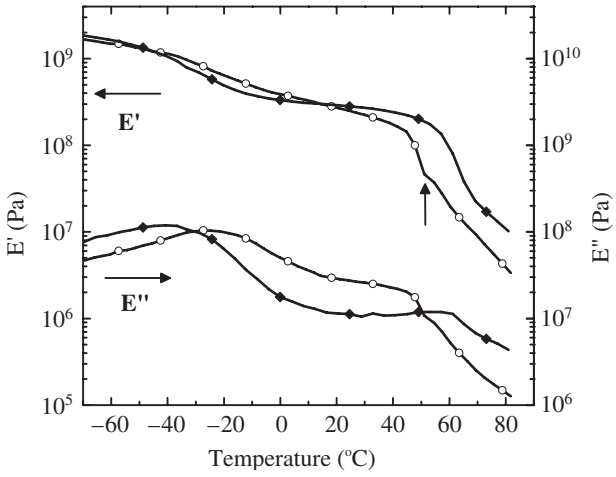

Fig. 11. Dynamic storage (E') and loss (E'') moduli vs. temperature obtained from DMTA at 1 Hz; samples stored at room temperature for 8 months prior to testing. (○) E/8AA/16*n*BA-45Mg, (♦) 65:35 ionomer : MgSt blend, fully neutralized. The arrow highlights the two-step modulus drop for the unmodified ionomer.

tails can contribute to the formation of rotator-type 'crystallites', while for MgOl and MgEr, only the polymer fraction of the blend is crystallizable. Indeed, the blend with MgSt has a higher storage modulus at 40 °C than does the unmodified ionomer, due to its higher overall level of 'crystallinity'; this is consistent with the higher Young's modulus evident in Fig. 1 at long aging times.

This is the key distinction between MgSt and MgOl or MgEr: while all form blends with very similar melt structures, only MgSt can crystallize to reinforce the material. However, unlike the previously-studied case of sulfonated ethylene–propylene–diene (SEPDM) ionomers blended with ZnSt [11,39,40], where ZnSt rapidly crystallizes out of the blend to form relatively large (order 100 nm) crystals [11,39], in our ionomer:MgSt blends, the MgSt tails order only slowly, to form structures which are comparable in size to the spacing between ionic aggregates. MgSt is thus an exceptionally effective 'filler' for E/(M)AA ionomers, especially those of low or zero crystallinity. When added to ionomers of higher crystallinity, such as those based on E/12AA, the initial suppression of primary crystallization acts counter to the reinforcing effect of the secondary crystals, leading to somewhat lower moduli even after long aging times for the blend vs. the unmodified ionomer (see third panel of Fig. 1).

3.3. Phase separation: ionomers blended with NaSt

Sodium stearate (NaSt) is a saturated, monovalent fatty acid salt often found in commercial soaps. Its thermal behavior and polymorphic liquid-crystalline structures have been thoroughly studied [41,42]. Unlike MgSt, anhydrous NaSt transforms through its polymorphs reversibly upon heating and cooling. Fig. 12 shows a series of DSC thermograms of the 39 wt% NaSt-modified ionomer taken at different aging times, as well as those of the pure ionomer and the pure NaSt. The many peaks observed in the NaSt trace above 120 °C reflect transitions between the various liquid-crystalline polymorphs of NaSt; the final transition, at 280 °C, represents the transition from the 'neat' phase to the isotropic phase [41,42]. For the blend, by contrast, no thermal activity other than decomposition is observed above 200 °C; SAXS measurements on the blend at 200 °C [26] reveal an isotropic structure similar to the blend SAXS pattern in Fig. 3 and the high-temperature blend pattern in Fig. 9. Thus, at the highest temperatures (200 °C and above), the NaSt and ionomer form a macroscopically single-phase material. However, at lower temperatures, the DSC curve for even the '0 h' blend shows endothermic transitions which clearly correspond to phase transitions in the pure NaSt (110 °C: transition to 'subwaxy' phase; 125 °C: transition to 'waxy' phase [41,42]). Thus, blends with NaSt more closely resemble the blends of SEPDM ionomers with ZnSt studied previously [11,39]: while the two components mix at sufficiently high temperatures, the stearate separates on cooling to form relatively large and pure domains. The remaining ionomer phase then behaves essentially as the pure ionomer does, forming primary crystals on initial cooling with a broad melting transition around 85 °C, and also forming secondary crystals on room-temperature storage which melt near 50 °C, as shown in Fig. 12. Indeed, the heat of melting for the secondary crystallites after 7 days of room-temperature aging corresponds to 61% of that of the pure ionomer with the same thermal history, identical to the ionomer's content in the blend, indicating that the two components are acting independently. The growth of these secondary crystals is responsible for the gradual modulus increase with room temperature aging evident in Fig. 1, but there is no coassembly between the two components, and no synergistic property modifications.

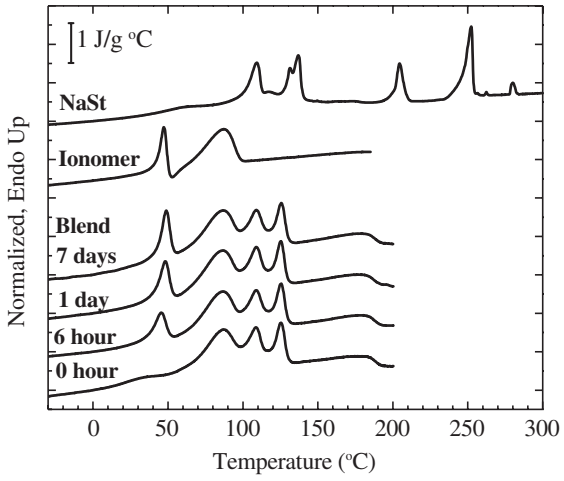

Fig. 12. Bottom: DSC thermograms of the fully-neutralized 61:39 E/19MAA ionomer:NaSt blend; time next to each curve refers to the period of room-temperature annealing following the quench from 200 °C. Top: heating traces for the pure components; NaSt after vacuum drying, and ionomer after 7 days of room-temperature following a quench from 150 °C, scaled by their respective weight fractions in the blend.

4. Conclusions

The morphology and properties of ionomer:metal soap blends depend subtly but crucially on the characteristics of the metal soap. For example, MgSt and MgOl are both salts of C_{18} fatty acids; both are fully miscible with E/(M)AA ionomers in the melt; and both induce a strong suppression of primary crystallization in the ionomer (though stronger for MgSt). But following an extended period of room-temperature aging, the physical properties of ionomer:MgSt and ionomer:MgOl blends can be radically different, since the alkyl tails in MgSt can 'crystallize' into a rotator structure while MgOl cannot. The metal cation employed also has a substantial impact on the phase behavior. While MgSt remains intimately mixed (coassembled) with the ionomer upon cooling, NaSt phase-separates to give a composite consisting of domains of essentially pure ionomer and NaSt, with no new solid-state structures or synergistic properties. Interestingly, while the blend behavior is quite sensitive to the metal soap chosen, it is relatively insensitive to the identity of the ionomer: though variations in acid type (MAA vs. AA), acid content, and termonomer content were all explored, all ionomers coassembled with the various metal soaps at sufficiently elevated

temperatures. The nature of the ionomer appears important only when comparing the solid-state properties of the unmodified ionomer against its blend with a metal soap (rather than when comparing the blends of a given ionomer with different metal soaps), and principally for the MgSt case. For ionomers of little or no crystallinity, blending with MgSt elevates the modulus (for well-aged specimens), due to the formation of the 'crystalline' rotator structure by MgSt, which can also incorporate ethylene sequences from the ionomer. However, for highly crystalline ionomers, blending with MgSt reduces the modulus, because the formation of rotator crystals on room-temperature storage cannot compensate for the suppression of primary crystallization.

Acknowledgements

DuPont Packaging and Industrial Polymers generously provided both financial support for this work and the materials studied herein. The authors are especially grateful to Brian Roach, Douglas Larson, Dr John Paul, Dr John Chen, and Dr George Prejean of DuPont for providing all the materials employed herein, often on demand. We also thank Mr Larson for the MI measurements, and especially Dr Chen for his guidance and stimulating discussions throughout.

References

[1] Eisenberg A, Kim J-S. Introduction to ionomers. New York: Wiley; 1998.
[2] Tant MR, Mauritz KA, Wilkes GL, editors. Ionomers: synthesis, structure, properties and applications. London: Blackie Academic and Professional; 1997.
[3] Longworth R. Thermoplastic ionic polymers: ionomers. In: Holliday L, editor. Ionic polymers. New York: Wiley; 1975. p. 69–172.
[4] Longworth R, Vaughan DJ. Nature 1968;218(5136):85–7.
[5] Register RA, Cooper SL. Macromolecules 1990;23(1):318–23.
[6] Wakabayashi K, Register RA. Macromolecules 2006;39(3):1079–86.
[7] Register RA, Prudhomme RK. Melt rheology. In: Tant MR, Mauritz KA, Wilkes GL, editors. Ionomers: synthesis, structure, properties and applications. London: Blackie Academic and Professional; 1997. p. 208–60.
[8] Bazuin CG. Plasticization studies of ionomers—a review. In: Utracki LA, Weiss RA, editors. Multiphase polymers: blends and ionomers (ACS symposium series 395). Washington: American Chemical Society; 1989. p. 476–502.
[9] Lundberg RD, Makowski HS, Westerman L. The dual plasticization of sulfonated polystyrene ionomer. In: Eisenberg A, editor. Ions in polymers (advances in chemistry series 187). Washington: American Chemical Society; 1980. p. 67–76.
[10] Weiss RA, Fitzgerald JJ, Kim D. Macromolecules 1991;24(5):1064–70.
[11] Jackson DA, Koberstein JT, Weiss RA. J Polym Sci, Part B: Polym Phys 1999;37(21):3141–50.
[12] Kim JS, Roberts SB, Eisenberg A, Moore RB. Macromolecules 1993; 26(19):5256–8.
[13] Orler EB, Gummaraju RV, Calhoun BH, Moore RB. Macromolecules 1999;32(4):1180–8.
[14] Plante M, Bazuin CG, Jerome R. Macromolecules 1995;28(5):1567–74.
[15] Tong X, Bazuin CG. Chem Mater 1992;4(2):370–7.
[16] Hara M, Jar P, Sauer JA. Polymer 1991;32(8):1380–3.
[17] Vorländer D. Chem Ber 1910;43(1):3120–35.
[18] Elliott SB. The alkaline earth and heavy-metal soaps. New York: Reinhold; 1946.
[19] Markley KS. Salts of fatty acids. In: Markley KS, editor. Fatty acids: their chemistry, properties, production, and uses, vol. 2. New York: Interscience; 1960. p. 715–56.
[20] Mehrotra RC, Bohra R. Metal carboxylates. London: Academic Press; 1983.
[21] Wunderlich B. Macromolecular physics. Crystal melting, vol. 3. New York: Academic Press; 1980.
[22] Adams JL, Quiram DJ, Graessley WW, Register RA, Marchand GR. Macromolecules 1996;29(8):2929–38.
[23] Register RA, Bell TR. J Polym Sci, Polym Phys Ed 1992;30(6):569–75.
[24] Annual book of ASTM standards, part 35. Philadelphia, PA: American Society for Testing and Materials; 1976. p. 427–37.
[25] Kohzaki M, Tsujita Y, Takizawa A, Kinoshita T. J Appl Polym Sci 1987; 33(7):2393–402.
[26] Wakabayashi K. PhD Thesis, Princeton University; 2006.
[27] Bracconi P, Andres C, Ndiaye A. Int J Pharm 2003;262(1-2):109–24.
[28] Spegt P, Skoulios A. C R Hebd Acad Sci 1962;254(25):4316–8.
[29] Vanhoorne P, Register RA. Macromolecules 1996;29(2):598–604.
[30] Tierney NK, Register RA. Macromolecules 2002;35(16):6284–90.
[31] Makowski HS, Brenner D, Bock J. US Patent 4,137,203, January 30, 1979, Exxon Research and Engineering Company.
[32] Yarusso DJ, Cooper SL. Polymer 1985;26(3):371–8.
[33] Loo YL, Wakabayashi K, Huang YE, Register RA, Hsiao BS. Polymer 2005;46(14):5118–24.
[34] Quiram DJ, Register RA, Ryan AJ. Macromolecules 1998;31(4):1432–5.
[35] Eisenberg A, Hird B, Moore RB. Macromolecules 1990;23(18): 4098–107.
[36] Akanni MS, Okoh EK, Burrows HD, Ellis HA. Thermochim Acta 1992; 208(1):1–41.
[37] Sharpe SA, Celik M, Newman AW, Brittain HG. Struct Chem 1997;8(1): 73–84.
[38] Sirota EB, King HE, Singer DM, Shao HH. J Chem Phys 1993;98(7): 5809–24.
[39] Duvdevani I, Lundberg RD, Wood-Cordova C, Wilkes GL. Modification of ionic associations by crystalline polar additives. In: Eisenberg A, Bailey FE, editors. Coulombic interactions in macromolecular systems (ACS symposium series 302). Washington: American Chemical Society; 1986. p. 184–200.
[40] Makowski HS, Lundberg RD. Plasticization of metal sulfonate-containing EPDM with stearic acid derivatives. In: Eisenberg A, editor. Ions in polymers (advances in chemistry series 187). Washington: American Chemical Society; 1980. p. 34–51.
[41] Skoulios A, Luzzati V. Nature 1959;183(4671):1310–2.
[42] Vold MJ, Macomber M, Vold RD. J Am Chem Soc 1941;63(1):168–75.